Research in Pharmaceutical Sciences, April 2021; 16(2): 217-226
Received: 17-05-2020
Peer Reviewed: 29-07-2020
Revised: 07-09-2020
Accepted: 20-02-2021
Published: 05-03-2021

School of Pharmacy & Pharmaceutical Sciences
Isfahan University of Medical Sciences

Original Article

Suppression of hypoxia and inflammatory pathways by *Phyllanthus niruri* extract inhibits angiogenesis in DMBA-induced breast cancer mice

Abu Hanifah Ramadhani[1], Ahmad Hafidul Ahkam[1], Aditya Ragil Suharto[2], Yoga Dwi Jatmiko[1], Hideo Tsuboi[3], and Muhaimin Rifa'i[1,*]

[1]Biology Department, Faculty of Mathematics and Natural Sciences, University of Brawijaya, Jl. Veteran Malang 65145, Malang, Indonesia.
[2]Department of Natural Resources Management, King Mongkut's University of Technology Thonburi, 126 Pracha Uthit Road, Bangkok 10140, Thailand.
[3]Department of Immunology, Nagoya University Graduate School of Medicine, 65 Tsurumai-cho, Showa-ku, Nagoya 466-8550, Japan.

Abstract

Background and purpose: Angiogenesis has been one of the hallmarks of cancer. In recent years, *Phyllanthus niruri* extract (PNE) was reported to inhibit angiogenesis by decreasing the levels of vascular endothelial growth factor (VEGF) and hypoxia-inducible factor-1α (HIF-1α) in breast cancer. However, the experimental results were confirmed in cancer cell lines only, whereas the anti-angiogenic activity in animal models has not been demonstrated. In this study, we tried to examine the anti-angiogenic activity of PNE on BALB/c strain mice models that were induced for breast cancer using the carcinogenic substance 7,12-dimethylbenz[a]anthracene (DMBA).
Experimental approach: Experimental animals were divided into five different groups; vehicle, DMBA, PNE 500 mg/kg, PNE 1000 mg/kg; and PNE 2000 mg/kg. Mammary carcinogenesis was induced using a subcutaneous injection of 15 mg/kg of DMBA for 12 weeks. Afterward, oral PNE treatment was given for the following 5 weeks. VEGFA and HIF-1α were observed using immunohistochemistry. Endothelial cell markers CD31, CD146, and CD34 were observed using the fluorescent immunohistochemistry method. The levels of interleukin-6 (IL-6), IL-17, and C-X-C motif chemokine (CXCL12) were measured using flow cytometry.
Findings/Results: The survival analysis indicated that PNE increased the survival rate of mice (P = 0.043, log-rank test) at all doses. The PNE treatment decreased the immunoreactive score of angiogenic factors (VEGF and HIF-1α), as well as the endothelial cell markers (CD31, CD146, and CD34). The PNE-treated groups also decreased the levels of inflammatory cytokines (IL-6, IL-17, and CXCL12) at all doses.
Conclusion and implications: This finding suggests that PNE may inhibit the progression of angiogenesis in breast cancer mice by targeting the hypoxia and inflammatory pathways.

Keywords: Angiogenesis; Breast cancer; DMBA; Inflammation; *Phyllanthus niruri.*

INTRODUCTION

Angiogenesis is the formation and elongation of pre-existing blood vessels. Although it is physiologically necessary for homeostasis, such as embryogenesis and wound healing, it is also a hallmark for cancer. Not only does it assist the tumor to metastasize, but also provides oxygen and nutrition to the growing tumor (1). The angiogenic factor vascular endothelial growth factor (VEGF) is among the most responsible factors to promote angiogenesis. One of the most substantial inducers of VEGF in the tumor microenvironment is hypoxia.

*Corresponding author: M. Rifa'i
Tel: +62-*341575841*, Fax: +62-341554 403
Email: *immunobiology@ub.ac.id*

Access this article online

Website: http://rps.mui.ac.ir

DOI: 10.4103/1735-5362.310528

Hypoxic cells in the tumor microenvironment stabilize hypoxia-inducible factor-1α (HIF-1α) and promote tumor angiogenesis by secreting VEGF into the extracellular matrix (2). Around 50-60% of tumors develop hypoxia and are heterogeneously distributed within the tumor microenvironment. Under normal conditions, the oxygen supply is adjusted to the tissue metabolic requirements. However, as a tumor develops, the oxygen consumption rate exceeds the oxygen availability, which then caused an imbalance in oxygen supply around the tissue. It was demonstrated that the partial oxygen pressure (pO2) in normal breast tissue is around 65 mmHg (1 mmHg = 133.3 Pa), while the pO2 within breast cancer tissue only reached 10 mmHg (3). Various infiltrating immune cells may also contribute to the aggressiveness of the tumor by promoting a vascular niche within the tissue. Cytokines such as interleukin-6 (IL-6) and IL-17 produced by immune cells also contribute to higher expression of VEGF (4). Furthermore, the chemokine C-X-C motif ligand (CXCL12) may enhance angiogenesis by recruiting progenitor endothelial cells, allowing blood vessels to penetrate the tumor microenvironment (5). These inflammatory events play a crucial role in the progression of angiogenesis.

The 7,12-dimethylbenz[a]anthracene (DMBA) is a polycyclic aromatic hydrocarbon with carcinogenic effects and has been successfully utilized to induce mammary tumors in rodents (6,7). The DMBA-induced breast cancer model had significantly high levels of inflammatory cytokines, such as IL-6, tumor necrosis factor alpha (TNF-α), interferon gamma (IFN-γ), and IL-1β (8). The underlying mechanisms of DMBA involve the mutation of the *ras* gene and cellular oxidative damage that were important for the development of cancer (9-11). To enhance tumorigenesis, DMBA was injected to young rodents when mammary glands are still undifferentiated and highly proliferative.

Remarkable antitumor responses were achieved by inhibiting angiogenesis. Therefore, clinically tested drugs were developed to inhibit VEGF and showed promising results (12). *Phyllanthus niruri* L. (*P. niruri*) is a traditional herb used by Asian people to treat several diseases such as malaria, hepatitis B, and diabetes (13). However, recent researches suggest anticancer effects in several cancer cell lines (14-16). Aqueous extract of *P. niruri* suppressed the tumor growth in DMBA-induced skin cancer mouse models without showing any toxic effects (17). It was speculated that *P. niruri* exhibits anticancer properties by regulating the expression of VEGFA and HIF-1α (18-20). Unfortunately, so far these studies were hypothesized using cancer cell lines only, and the anti-angiogenic activity of *P. niruri* in animal models has not been validated. In this study, we investigated the therapeutic effects of *P. niruri* in animal models to confirm the anti-angiogenic activity in breast cancer.

MATERIALS AND METHODS

Herb extraction

P. niruri (Specimen No. 075/84A/102.7/2019) was obtained and identified from UPT Materia Medika (Batu City, Indonesia). Herb extraction was prepared by dissolving grounded herb powder with distilled aqua with a 1:10 ratio (herb:solvent, w/v). The solution was shaken using a rotary shaker at 1000 rpm for 24 h. The filtered mixture was evaporated and freeze-dried at -20 °C for one week to remove the remaining water. *P. niruri* extract (PNE) was kept at 4 °C freezer for storage.

Experimental design

All procedures in this experiment were evaluated and proved by the Animal Care and Use Committee from the University of Brawijaya (Ethic No. 1152-KEP-UB). Experiments were carried out with 7-week-old female BALB/c mice obtained from Gajah Mada University, Yogyakarta, Indonesia, n = 75. The animals were kept in a standard pathogen-free facility and had free access to food and water. After a week of acclimatization, the animals were randomly separated into 5 different groups. Vehicle group, mice were neither exposed to DMBA nor given any PNE treatment (n = 15); DMBA group, mice were exposed to 15 mg/kg DMBA without given any PNE treatment (n = 15); PNE

groups, mice were exposed with 15 mg/kg DMBA and were treated with 3 different doses of PNE at 500, 1000, and 2000 mg/kg (n = 15, for each respective dose). These doses were previously tested for acute toxicity tests to healthy mice for 14 days but did not cause any mortality (data were not shown). Breast cancer was induced using multiple doses of DMBA (Tokyo Chemical Industry, Japan) injected subcutaneously in the mammary glands. The injection was done weekly for 12 weeks and was then given daily oral PNE treatment for 5 weeks. Due to the high toxicity of DMBA, not all mice survived until the end of the study, and these mice were not counted in our data analysis except for survival analysis only. In this case, at least 5 mice must remain in each group for data analysis.

Histological analysis

Hematoxylin and eosin staining

Dissected breast tissue was immersed in 10% neutral-buffered formalin for 24 h at room temperature. Fixated tissue was then dehydrated, embedded in paraffin, and then sectioned to 5 µm thick. Sections were stained with hematoxylin and eosin (H&E) and mounted on top of slides.

Immunohistochemistry staining

Histological slides were rehydrated and endogenous enzymes were blocked with 3% peroxidase for 40 min. Antigen retrieval was done by immersing slides with 0.01 M pH 6 citrate buffer at 90 °C for 5 min. Background staining was blocked with Superblock™ blocking buffer (Thermo Fisher Scientific, USA) for 30 min. Sections were diluted with primary antibodies rabbit anti-HIF-1α and anti-VEGFA (Santa Cruz Biotechnology, USA) overnight at 4 °C and incubated with horseradish peroxidase-conjugated goat anti-mouse secondary antibody (Santa Cruz Biotechnology, USA) for 30 min. Slides were diluted with 3,3'-diaminobenzidine (DAB) as a chromogenic substance for 2 min. Mayer's hematoxylin was used as a counter-stain.

Fluorescent immunohistochemistry staining

Fluorescent staining was done using a direct method to utilize three antibodies altogether. The antibodies include Alexa Fluor 405-conjugated anti-cluster of differentiation (CD) 31, FITC-conjugated anti-CD146, and PE-conjugated anti-CD34 (BioLegend, USA). Dissected tissue was rehydrated in xylene, descending grades of ethanol, and finally in distilled water. Endogenous enzymes were blocked with 3% peroxidase for 40 min and incubated with Superblock™ blocking buffer for 30 min. Sections were diluted with fluorochrome-conjugated primary antibodies for 60 min at 4 °C, mounted with anti-fade mounting media, and were immediately examined.

Flow cytometry

The antibodies used include PE-conjugated anti-CD4, FITC-conjugated anti-CD68, PE/Cy5.5-conjugated anti-IL-6, PerCP/Cy5.5-conjugated anti-IL-17, and PerCP/Cy5.5-conjugated anti-CXCL12 (BioLegend, USA). The spleen was isolated and homogenized with phosphate buffer saline (PBS). Homogenate was centrifuged (2500 rpm, 10 °C, 5 min), and the cell suspension was stained with 50 µL extracellular antibodies (anti-CD4 and anti-CD68). Intracellular staining was performed by applying 50 µL Cytofix^{TM} (BD-Biosciences Pharmingen) and wash perm solution (BioLegend, USA) for permeabilization. After centrifugation (2500 rpm, 10 °C, 10 min), the cells were stained with intracellular antibodies of the target (anti-IL-6, anti-IL-17, and anti-CXCL12). The sample was added with 400 µL of PBS, and was subjected to flow cytometry analysis (BD FACSCalibur, USA) according to Rifa'i *et al*. (21). No stimulators of cytokines were used during the flow cytometry method.

Immunohistochemistry scoring

Analysis of immunohistochemistry was semi-quantitatively using the immunoreactivity scoring system according to Vijayashree *et al.* (22). The intensity was scored as 0 (no stain), 1 (weak stain), 2 (moderate stain), and 3 (strong stain). Percentage of cells was scored as 0 (none), 1 (< 10%), 2 (10-50%), 3 (51-80%), and 4 (> 80%). The total immunoreactivity score was calculated by multiplying intensity score with percentage cell score ranging from 0 to 12.

Statistical analysis

Survival curves were estimated by the Kaplan-Meier method and evaluated with the log-rank test. Statistics for flow cytometry and immunohistochemical staining were analyzed for ANOVA test and post-hoc Tukey HSD test using SPSS 25.0 software (SPSS Inc., Chicago, Illinois). In this study, a value of $P < 0.05$ was considered significant between two different groups. All data were shown in mean ± standard deviation (SD).

RESULTS

Mortality and survival analysis

The exposure of DMBA was highly toxic and caused a 67% mortality rate in the DMBA group until the end of the study. However, the mice receiving 500, 1000, and 2000 mg/kg of PNE treatment had a lower mortality rate with 33%, 26%, and 20%, respectively. In contrast, all mice in the vehicle group survived until the end of the experiment. Based on the Kaplan-Meier survival analysis, PNE treatment had a higher survival rate compared to the DMBA group ($P = 0.043$, Fig. 1). As the survival function goes higher, we also observed a significant reduction in the hazard rate post-treatment. These data suggest that PNE had a better chance of survival after being induced for breast cancer using DMBA.

Immunohistochemical staining of angiogenic proteins

The breast tissue was primarily composed of lipid cells, glandular epithelial cells, and connective tissue (Fig. 2). We noticed the infiltration of immune cells between the epithelial cells and lipid cells. Vascularization of blood vessels and hyperplasia ductal epithelial cells were also observed. The expression of angiogenic factors on breast tissue was observed using immunohistochemistry and was analyzed for immunoreactive score (Fig. 3A). Compared to the vehicle group, the DMBA group had significantly higher levels of HIF-1α and VEGFA, which scored 10.2 ($P < 0.001$) and 10.6 ($P < 0.001$), respectively. The treatment of PNE had a lower score of HIF-1α and VEGFA, suggesting a potential suppression by the treatment. Furthermore, PNE at 2000 mg/kg showed the highest suppressive effect by reducing the score to 6 ($P < 0.001$) and 7.8 ($P < 0.01$), respectively.

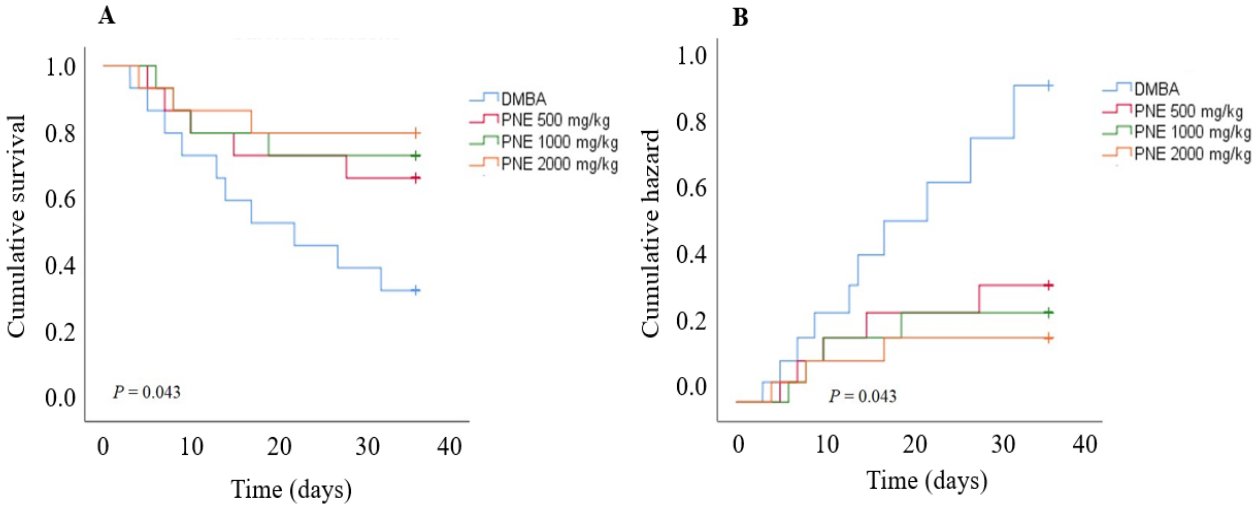

Fig. 1. Kaplan-Meier analysis was measured for 5 weeks after receiving PNE treatment. Mice were exposed to DMBA for 12 weeks prior to the treatment. (A) The survival analysis showed that the mice treated with PNE had a better chance of survival. (B) Similarly, the hazard function also reveals that treated mice had a lower hazard rate compared to the DMBA group. DMBA, 7,12-dimethylbenz[a]anthracene; PNE, *Phyllanthus niruri* extract.

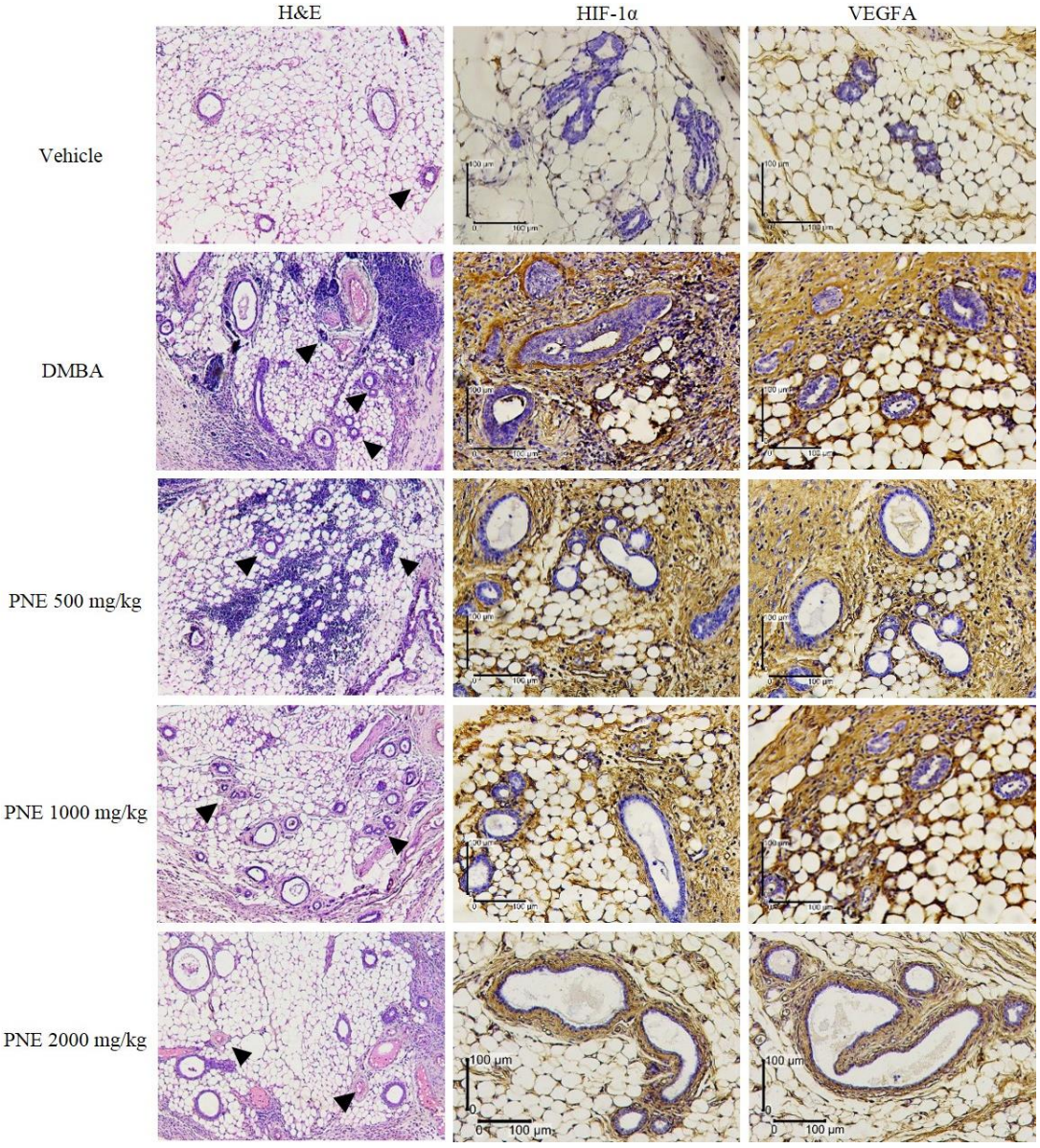

Fig. 2. H&E staining reveals blood vessels (arrowheads) that grow in mammary tissue. The expression of HIF-1α and VEGFA were observed using immunohistochemistry staining. DMBA, 7,12-Dimethylbenz[a]anthracene; H&E, hematoxylin and eosin; HIF, hypoxia-inducible factor; PNE, *Phyllanthus niruri* extract; VEGFA, vascular endothelial growth factor A.

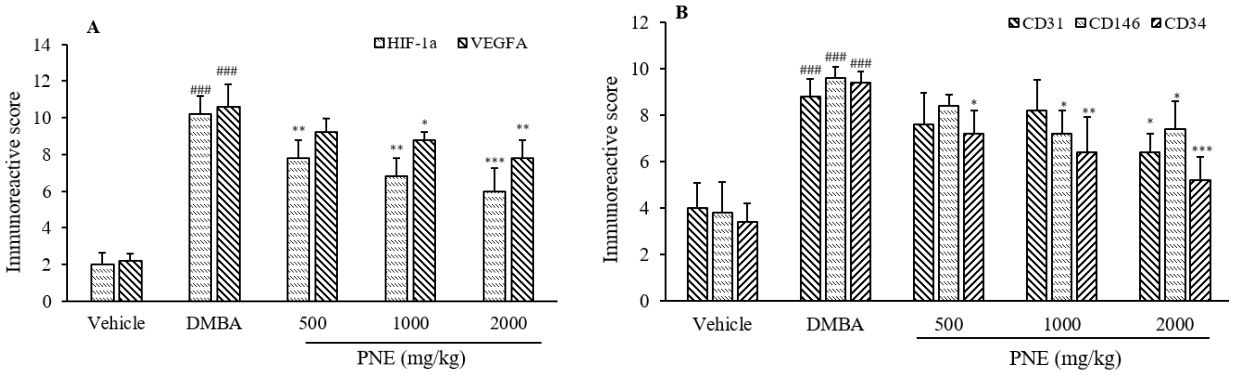

Fig. 3. Immunoreactive score of (A) angiogenic factors and (B) endothelial cell markers. Scores range from 0-12. $^{###}P < 0.001$ indicates significant difference compared to the vehicle group; $^{*}P < 0.05$, $^{**}P < 0.01$, $^{***}P < 0.001$ versus DMBA group. CD, Cluster of differentiation; DMBA, 7,12-dimethylbenz[a]anthracene; HIF, hypoxia inducible factor; PNE, *Phyllanthus niruri* extract; VEGFA, vascular endothelial growth factor A.

Fluorescent immunohistochemical staining of endothelial cell markers

In this study, we used CD31, CD146, and CD34 to stain endothelial cell markers in breast tissue (Fig. 4). Based on the immunoreactive score, the expression of CD31, CD146, and CD34 in DMBA group was significantly (P < 0.001) higher than the vehicle group, which scored 8.8, 9.6, and 9.4, respectively (Fig. 3B). The groups that received PNE treatment had scored lower than the DMBA group. PNE at 2000 mg/kg had the highest suppressive effect, which reduced the score of CD31, CD146, and CD34 to 6.4 (P < 0.05), 7.4 (P < 0.05), and 5.2 (P < 0.001), respectively.

Flow cytometric analysis of cytokines and chemokine

Since angiogenesis is correlated with inflammatory cytokines, we further analyzed IL-6 expressed from CD68 cells, IL-17 expressed from CD4 cells, and CXCL12 expressed in all cell populations (Fig. 5). Compared to the vehicle group, the DMBA group had significantly (P < 0.001) higher levels of IL-6, IL-17, and CXCL12 with 9.168%, 2.027%, and 2.076%, respectively. However, the treatment of PNE significantly decreased the levels of IL-6, IL-17, and CXCL12 at all doses.

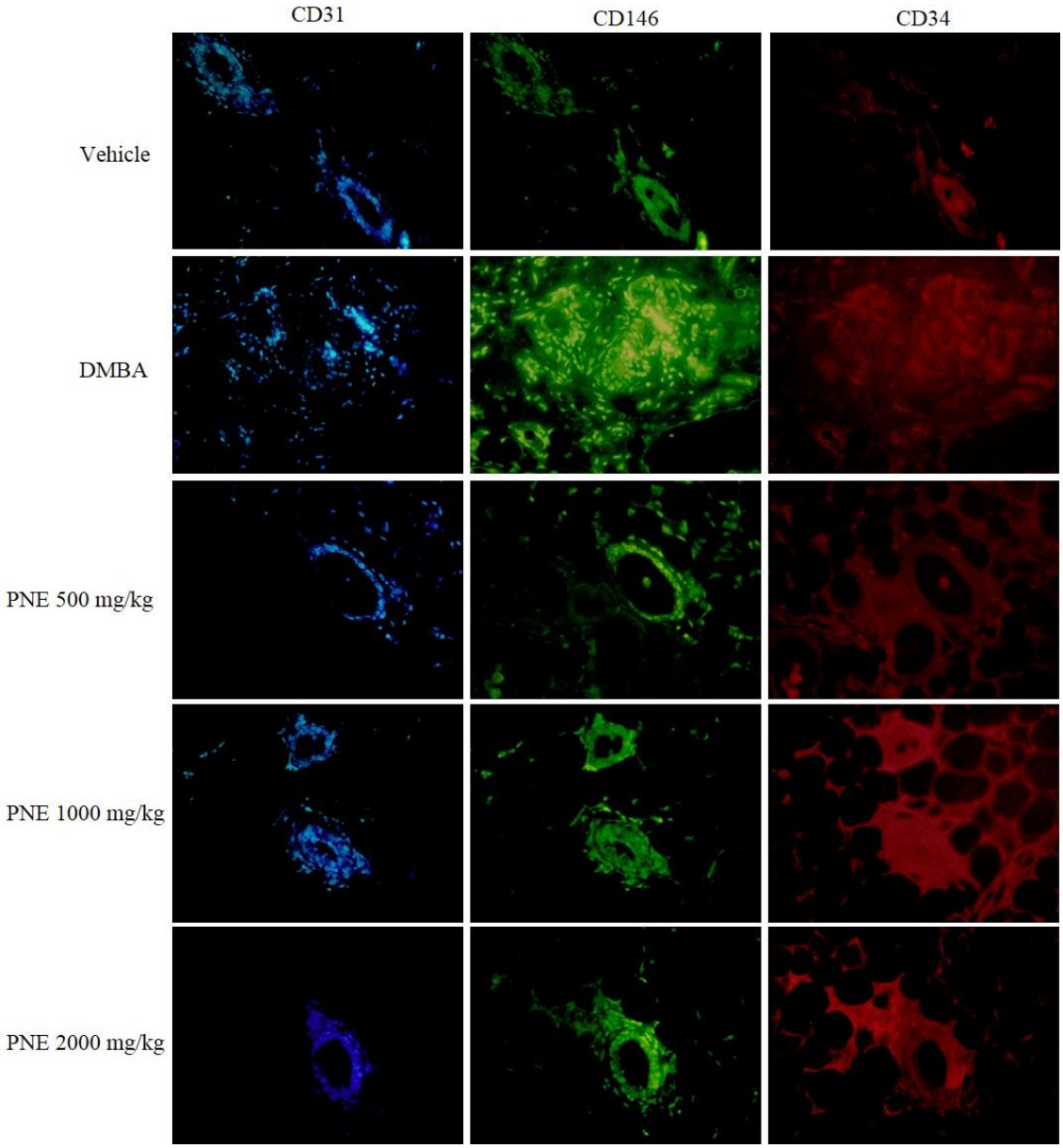

Fig. 4. Fluorescent immunohistochemical staining of endothelial cell markers. The expression of CD31, CD146, and CD34 were marked by blue, green, and red, respectively. CD, Cluster of differentiation; DMBA, 7,12-dimethylbenz[a]anthracene; PNE, *Phyllanthus niruri* extract.

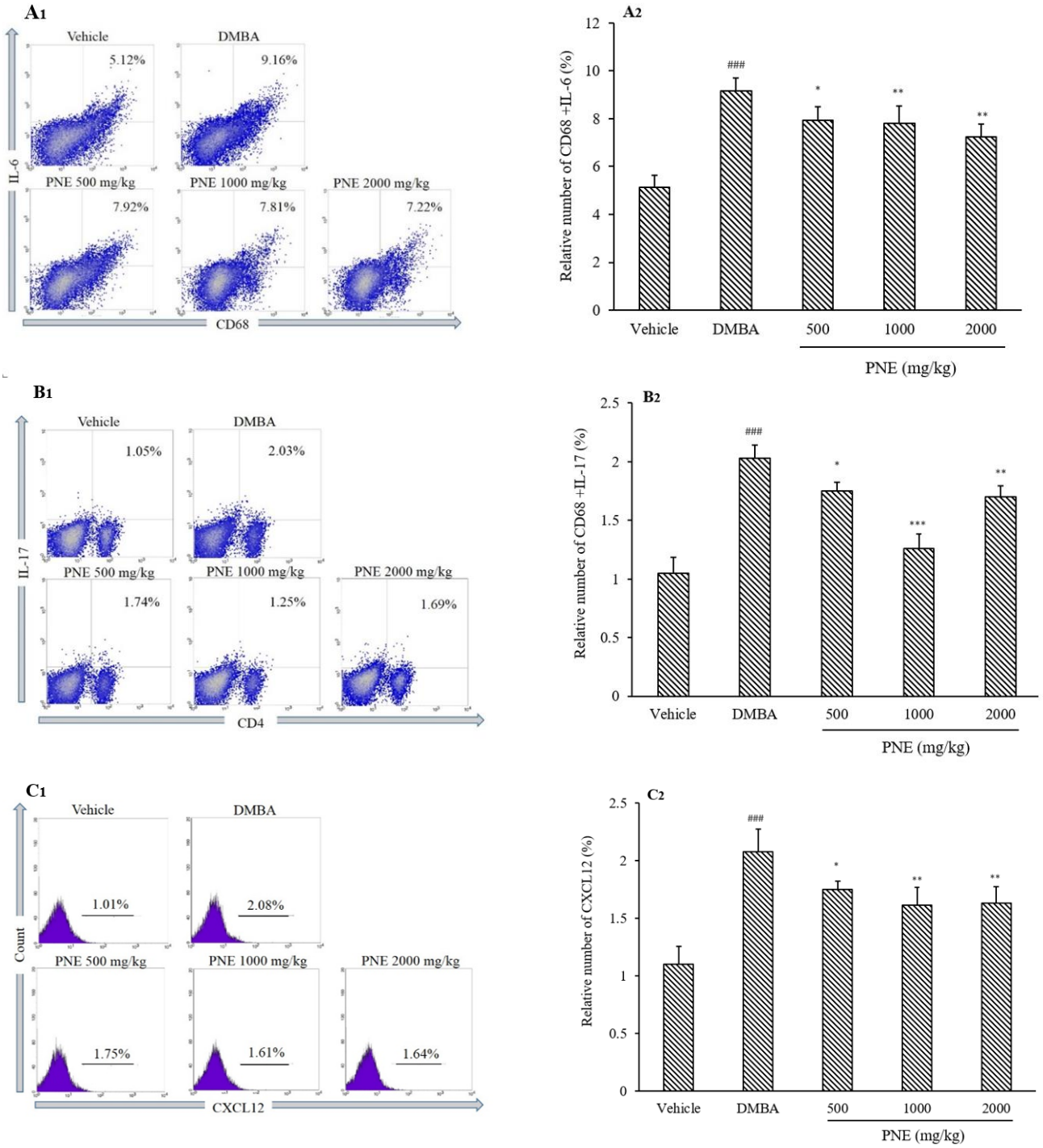

Fig. 5. Flow cytometry analysis of (A) IL-6, (B) IL-17, and (C) CXCL12. All data represent mean ± SD. $^{###}P < 0.001$ indicates significant difference compared to the vehicle group; $^{*}P < 0.05$, $^{**}P < 0.01$, $^{***}P < 0.001$ in contrast to DMBA group. CD, Cluster of differentiation; DMBA, 7,12-dimethylbenz[a]anthracene; IL, interleukin; PNE, *Phyllanthus niruri* extract.

DISCUSSION

A previous study reported that the median acute toxicity (LD_{50}) of PNE administered to Swiss albino mice was 2600 mg/kg, which suggests that PNE may cause mortality in healthy mice (23). However, in our study, we did not observe any mortality in healthy mice receiving up to 2000 mg/kg dose of PNE after 14 days of administration. Instead of showing any signs of toxicity, the oral treatment of PNE had given a significant impact on the animal's survival. Fewer skin lesions were observed, and the mice gained more body weight as they had a better appetite. While there was a 67% mortality rate in the DMBA group, the PNE-

treated groups had a significantly lower mortality rate that can be observed in a dose-dependent manner. On the contrary, the vehicle group that was not exposed to DMBA or given any PNE treatment survived until the end of the study.

VEGF is a key factor in the formation of new blood vessels. While the expression of VEGF may be derived from various factors, hypoxia is considered to be one of the substantial inducers for VEGF. In this study, we found that PNE treatment significantly reduced the expression of HIF-1α and VEGF in a dose-dependent manner. Based on the immunohistochemical analysis, these angiogenic factors were highly expressed in the tumor microenvironment and showed a poor prognosis towards the animal's survival. The downregulation of VEGF may be caused by the reduction of HIF-1α, indicating less severity of hypoxia within the tissue. It was also worth noting that the expression of VEGF scored higher than HIF-1α, demonstrating that VEGF had higher expression than HIF-1α. A previous study reported that PNE inhibits VEGF in the MCF-7 breast cancer cell line by downregulating HIF-1α in the hypoxia pathway (20). Another study using the PC3 and MeWo cell lines also achieved similar results, which further supports the hypothesis that PNE may inhibit the hypoxia pathways in cancer (18,19). Apart from downregulating HIF-1α and PNE also inhibits tumorigenesis by altering the mitogen-activated protein kinase (MAPKs), phosphoinositide 3-kinases/protein kinase B (PI3K/Akt), and nuclear factor kappa (NFκB) pathways, which leads to the suppression of tumor proliferation. Not only does it suppress metastasis, but it also induces selective killing among cancer cell lines, allowing specific-targeted apoptosis without killing normal cells. Based on the phytochemical constituents, several compounds from *P. niruri* were proposed to be responsible for the anticancer properties. They include gallic acid, galloylglucopyranoside, corilagin, geraniin, rutin, quercetin glucoside, caffeolquinic acid, and digalloylglucopyranoside (14,15,16).

In the present study, the progression of angiogenesis was marked by the immunoreactive score of CD31, CD146, and CD34. In general, these markers were commonly used to detect vascular blood vessels in mice. Here we showed that all doses of PNE treatment significantly reduced the score of CD34, a popular pan marker for stem cells. The CD146 marker was significantly reduced at 1000 and 2000 mg/kg, whereas the 500 mg/kg dose did not significantly reduce the score. On the contrary, the score of CD31 marker was relatively difficult to diminish, since it was only significantly decreased at 2000 mg/kg dose. Therefore, we imply that the reduction of endothelial cell markers correlates with the decrement of angiogenic factors as previously described. This illustrates the inhibition of angiogenic factors may suppress the formation of blood vessels in breast tissues. CD31 is highly expressed by vascular endothelial cells and was involved in angiogenesis, immune escape, and tumor growth (24). Similarly, CD146 was regarded as one of the pan markers of endothelial cells in mice and was mainly expressed at the junction between endothelial cells and directly interacts with VEGFR-2 (25,26). CD34 was commonly used as a marker for hematopoietic stem cells and hematopoietic progenitor cells. However, CD34 can also serve as a marker for other nonhematopoietic cell types, such as vascular endothelial progenitors and embryonic fibroblasts (27).

Although PNE significantly suppressed angiogenic factors, the underlying mechanisms remain unclear. Here we tried to examine the effects of PNE treatment against inflammatory cytokine and chemokine that were responsible for promoting angiogenesis. Based on the aforementioned results, we observed a significant reduction of IL-6, IL-17, and CXCL12 in mice receiving PNE treatment compared to the DMBA group. The cytokines were reduced at all doses, but the highest suppressive effect was observed in the 1000 mg/kg dose. The DMBA-induced breast cancer model may upregulate the expression of IL-6, TNF-α, IFN-γ, and IL-1β produced by macrophages. Furthermore, it may also trigger the activation of CD4 and CD8 T cells by losing the L-selectin (CD162L) marker (8). There weren't many studies of PNE evaluating the inflammatory cytokines in breast cancer models, but there have been studies suggesting the potent anti-inflammatory properties of PNE

(13). The compound corilagin was demonstrated to inhibit the secretion of TNF-α, IL-1β, IL-6, NO (iNOS), and COX-2 at the protein and gene level (28).

CONCLUSION

The administration of DMBA displayed several hallmarks of cancer, including inflammation, hypoxia, and an increase in tissue vascularization. The groups treated with *P. niruri* extract showed a significant reduction in the expression of angiogenic factors, endothelial cell markers, as well as inflammatory cytokines. In general, these groups also acquire a better chance of survival compared to the untreated group. Our findings suggest that the herb may inhibit the progression of angiogenesis in the breast cancer model. Since there were plentiful reports about the antitumor activity of *P. niruri*, it is suggested that more research should be put to understand the mechanism and its therapeutic effects.

Conflict of interest statement

The authors declared no conflict of interest in this study.

Acknowledgments

This research was financially supported by the Ministry of Research, Technology, and Higher Education of Republic Indonesia (Grant No. 063/ADD/SP2H/LT/DPRM/VIII/2017).

Authors' contribution

A.H. Ramadhani conducted the research, analyzed the data, and wrote the manuscript. A.H. Ahkam and A.R. Suharto conducted the research. Y.D. Jatmiko and H. Tsuboi supervised the project and revised the manuscript. M. Rifa'i designed the experiment, provided financial support, and reviewed the manuscript.

REFERENCES

1. Gatenby RA, Gillies RJ. Why do cancers have high aerobic glycolysis? Nat Rev Cancer. 2004;4(11):891-899.
   DOI: 10.1038/nrc1478.
2. Potente M, Gerhardt H, Carmeliet P. Basic and therapeutic aspects of angiogenesis. Cell. 2011;146(6):873-887.
   DOI: 10.1016/j.cell.2011.08.039.
3. Vaupel P, Höckel M, Mayer A. Detection and characterization of tumor hypoxia using pO2 histography. Antioxid Redox Signal. 2007;9(8):1221-1235.
   DOI: 10.1089/ars.2007.1628.
4. Murugaiyan G, Saha B. Protumor *vs* antitumor functions of IL-17. J Immunol. 2009;183(7):4169-4175.
   DOI: 10.4049/jimmunol.0901017.
5. Sun X, Cheng G, Hao M, Zheng J, Zhou X, Zhang J, *et al*. CXCL12/CXCR4/CXCR7 chemokine axis and cancer progression. Cancer Metastasis Rev. 2010;29(4):709-722.
   DOI: 10.1007/s10555-010-9256-x.
6. Burchiel SW, De Ann PD, Gomez MP, Montano RM, Barton SL, Seamer LC. Inhibition of lymphocyte activation in splenic and gut-associated lymphoid tissues following oral exposure of mice to 7,12-dimethylbenz[a]anthracene. Toxicol Appl Pharmacol. 1990;105:434-442.
   DOI: 10.1016/0041-008X(90)90147-M.
7. Buters J, Quintanilla-Martinez L, Schober W, Soballa VJ, Hintermair J, Wolff T, *et al*. CYP1B1 determines susceptibility to low doses of 7,12-dimethylbenz[a]anthracene-induced ovarian cancers in mice: correlation of CYP1B1-mediated DNA adducts with carcinogenicity. Carcinogenesis. 2003;24(2):327-334.
   DOI: 10.1093/carcin/24.2.327.
8. Ramadhani AH, Nafisah W, Isnanto H, Sholeha TK, Jatmiko YD, Tsuboi H, *et al*. Immunomodulatory effects of *Cyperus rotundus* extract on 7,12-dimethylbenz[a]anthracene (DMBA) exposed BALB/c mice. Pharm Sci. 2020;27(1):46-55.
   DOI: 10.34172/PS.2020.61.
9. Balmain A, Harris CC. Carcinogenesis in mouse and human cells: parallels and paradoxes. Carcinogenesis. 2000;21(3):371-377.
   DOI: 10.1093/carcin/21.3.371.
10. Currier N, Solomon SE, Demicco EG, Chang DLF, Farago M, Ying H, *et al*. Oncogenic signaling pathways activated in DMBA-induced mouse mammary tumors. Toxicol Pathol. 2005;33(6):726-737.
    DOI: 10.1080/01926230500352226.
11. Arulkumaran S, Ramprasath VR, Shanthi P, Sachdanandam P. Restorative effect of Kalpaamruthaa, an indigenous preparation, on oxidative damage in mammary gland mitochondrial fraction in experimental mammary carcinoma. Mol Cell Biochem. 2006;291(1-2):77-82.
    DOI: 10.1007/s11010-006-9199-2.
12. Kuczynski EA, Vermeulen PB, Pezzella F, Kerbel RS, Reynolds AR. Vessel co-option in cancer. Nat Rev Clin Oncol. 2019;16(8):469-493.
    DOI: 10.1038/s41571-019-0181-9.
13. Kaur N, Kaur B, Sirhindi G. Phytochemistry and pharmacology of *Phyllanthus niruri* L.: a review. Phytother Res. 2017;31(7):980-1004.
    DOI: 10.1002/ptr.5825.

14. Tang YQ, Jaganath IB, Sekaran SD. *Phyllanthus spp*. induces selective growth inhibition of PC-3 and MeWo human cancer cells through modulation of cell cycle and induction of apoptosis. PLoS One. 2010;5(9):e12644,1-11.
DOI: 10.1371/journal.pone.0012644.
15. Lee SH, Jaganath IB, Wang SM, Sekaran SD. Antimetastatic effects of *Phyllanthus* on human lung (A549) and breast (MCF-7) cancer cell lines. PLoS One. 2011;6(6):e20994,1-14.
DOI: 10.1371/journal.pone.0020994.
16. Júnior RFDA, Soares LAL, da Costa Porto CR, de Aquino RGF, Guedes HG, Petrovick PR, *et al*. Growth inhibitory effects of *Phyllanthus niruri* extracts in combination with cisplatin on cancer cell lines. World J Gastroenterol. 2012;18(31):4162-4168.
DOI: 10.3748/wjg.v18.i31.4162.
17. Sharma P, Parmar J, Verma P, Sharma P, Goyal PK. Anti-tumor activity of *Phyllanthus niruri* (a medicinal plant) on chemical-induced skin carcinogenesis in mice. Asian Pac J Cancer Prev. 2009;10(6):1089-1094.
18. Tang YQ, Jaganath IB, Manikam R, Sekaran SD. *Phyllanthus* suppresses prostate cancer cell, PC-3, proliferation and induces apoptosis through multiple signaling pathways (MAPKs, PI3K/Akt, NF*κ*B, and Hypoxia). Evid Based Complement Alternat Med. 2013;2013:609581,1-13.
DOI: 10.1155/2013/609581.
19. Tang YQ, Jaganath IB, Manikam R, Sekaran SD. Inhibition of MAPKs, Myc/Max, NFκB, and Hypoxia pathways by *Phyllanthus* prevent proliferation, metastasis, and angiogenesis in human melanoma (MeWo) cancer cell line. Int J Med Sci. 2014;11(6):564-577.
DOI: 10.7150/ijms.7704.
20. Lee SH, Jaganath IB, Atiya N, Manikam R, Sekaran SD. Suppression of ERK1/2 and hypoxia pathways by four *Phyllanthus species* inhibits metastasis of human breast cancer cells. J Food Drug Anal. 2016;24(4):855-865.
DOI: 10.1016/j.jfda.2016.03.010.
21. Rifa'i M, Widodo N. Significance of propolis administration for homeostasis of CD4+CD25+ immunoregulatory T cells controlling hyperglycemia. Springerplus. 2014;3:526-533.
DOI: 10.1186/2193-1801-3-526.
22. Vijayashree R, Aruthra P, Ramesh Rao K. A Comparison of manual and automated methods of quantitation of oestrogen/progesterone receptor expression in breast carcinoma. J Clin Diagn Res. 2015;9(3):EC01-EC05.
DOI: 10.7860/JCDR/2015/12432.5628.
23. Singh T, Singh A, Kumar R, Singh JK. Acute toxicity study of *Phyllanthus niruri* and its effect on the cyto-architectural structure of nephrocytes in Swiss albino mice Mus-musculus. Pharmacogn J. 2016;8(1):77-80.
DOI: 10.5530/pj.2016.1.17.
24. Cao G, O'Brien CD, Zhou Z, Sanders SM, Greenbaum JN, Makrigiannakis A, *et al*. Involvement of human PECAM-1 in angiogenesis and *in vitro* endothelial cell migration. Am J Physiol Cell Physiol. 2002;282(5):C1181-C1190.
DOI: 10.1152/ajpcell.00524.2001.
25. Stalin J, Harhouri K, Hubert L, Subrini C, Lafitte D, Lissitzky JC, *et al*. Soluble melanoma cell adhesion molecule (smcam/scd146) promotes angiogenic effects on endothelial progenitor cells through angiomotin. J Bio Chem. 2013;288(13):8991-9000.
DOI: 10.1074/jbc.M112.446518.
26. Shih LM, Hsu MY, Palazzo JP, Herlyn M. The cell-cell adhesion receptor Mel-CAM acts as a tumor suppressor in breast carcinoma. Am J Pathol. 1997;151(3):745-751.
27. Sidney LE, Branch MJ, Dunphy SE, Dua HS, Andrew H. Concise review: evidence for CD34 as a common marker for diverse progenitors. Stem Cells. 2014;32(6):1380-1389.
DOI: 10.1002/stem.1661.
28. Zhao L, Zhang SL, Tao JY, Pang R, Jin F, Guo Y, *et al*. Preliminary exploration on anti-inflammatory mechanism of Corilagin (beta-1-O-galloyl-3,6-(R)-hexahydroxydiphenoyl-D-glucose) *in vitro*. Int Immunopharmacol. 2008;8(7):1059-1064.
DOI: 10.1016/j.intimp.2008.03.003.